PREDICTION OF CREEP TRANSIENTS IN ZIRCALOY FUEL CLADDING USING ANELASTIC STRAIN MODEL

K. L. MURTY, K. K. YOON

Babcock & Wilcox Company, Lynchburg Research Center,
P.O. Box 1260, Lynchburg, Virginia 24505, U.S.A.

ABSTRACT

Nuclear fuel cladding tubes are subject, in service, to complex multiaxial loading that might undergo sudden changes. An accurate description of the strain response due to this transient behavior is essential in reliably predicting the accumulated plastic strains in the cladding. Direct extrapolations of the creep behavior under constant load to describe creep under varying loads result in significantly larger strains than observed, mainly due to the negative (inverse) transients following load drops.

The model equations developed in the past by Murty, et al., were based on the climb-controlled dislocation slip and were shown to successfully predict the creep behavior of Zircaloy cladding under a given set of constant loading conditions. Variations in any of the test variables, especially stress during a creep test produce "transients" following the sudden change; in particular, negative creep (contraction) results following a significant drop in the applied stress. These creep equations in their present form cannot account for this transient behavior.

In the pesent extensions of the models above, the transients following load changes are described following Hart, et al., using short-term anelastic deformation. Hoop creep tests were carried out at 750F on closed-end, internally pressurized, cold-worked, stress-relieved Zircaloy-4 caldding. Internal pressure was suddenly changed while continuously monitoring the hoop strain. Experimental data revealed inverse transients following significant decrease in the stress, while reduced normal primary creep was noted due to stress increase. Using the various constants experimentally evaluated from constant-stress creep and load relaxation data, a good correlation was noted between the experimental and predicted strains. The model predicted the negative creep following stress drop as observed experimentally.

Applications of the presently proposed model equations for predicting the multiaxial creep behavior as well as creep due to cyclic loading are discussed.

1. Introduction

Nuclear fuel cladding tubes are subject, in service, to complex multiaxial loading that undergoes sudden changes. Principal factors contributing to the stresses on Zircaloy tubing are the external pressure of the coolant, the internal pressure due to the released fission gas buildup, and, after sufficient burnup, the pellet-cladding mechanical interaction (PCMI). An accurate description of the strain response due to these varying applied stresses and temperature is essential in reliabily predicting the accumulated plastic strains in the cladding. Direct extrapolations of the creep behavior under constant load to describe creep under varying loads would result in significantly different strains than observed, mainly due to the inverse (negative) transients following load drops.

The model equations developed in the past by Murty, et al. [1] were based on the climb-controlled dislocation slip and were shown to successfully predict the creep behavior of Zircaloy cladding under a given set of constant loading conditions. Variations in any of the test variables, especially stress, during creep produces "transients" following the sudden change; in particular, negative creep (contraction) results following a significant drop in the applied stress (although the sign of the stress is unchanged. [2] In the present extensions of these models, the transients due to load changes are described following the ideas of Hart and coworkers [3,4] using short-term anelastic deformation [5]. A strain-hardening rule (in lieu of time-hardening) was used in evaluating the plastic strain following the stress change.

The model predictions were compared with the experimental data, and excellent correlations were noted. The applicability of the presently proposed model equations to describe creep under cyclic loading was demonstrated, and extensions of the present models to anisotropic multiaxial creep behavior under varying multiaxial loads are outlined.

2. Creep Under Constant Loading

The main data base, from which the model equations were developed to describe the temperature and stress dependencies of creep, was obtained using interrupted internal pressurization tests [1]. Experimental details and data analyses are detailed in [1], and a brief description of the model equations is included here. Correlations were developed from the pressure creep data [1] ranging from hoop stresses of 10 ksi (68.95 MPa) to 26 ksi (172.38 MPa) at temperatures from 600 to 800F (588.6 to 699.7K). From the temperature dependence of the minimum or steady-state creep rates at a constant applied hoop stress, a value of 64 kcal/mole (2.78 eV) was evaluated for the activation energy for creep. This value compares with that for self-diffusion in Zr-1.3% Sn of 62 kcal/mole (2.69 eV) determined by Lyashenko [6].

The close agreement of the activation energy for creep and that for self-diffusion suggests a diffusion-controlled creep mechanism. Using Dorn's quasi-theoretical approach [7], the experimental data were shown to fit the following creep equation [1]:

$$\dot{\varepsilon}_\theta^s = A_1 \frac{DEb}{kT} \exp(B_1 \sigma_\theta / E) \qquad (1)$$

where A and B are material constants, $D[= D_o \exp(Q_D/RT)]$ the self-diffusion coefficient with an activation energy of Q_D (62 kcal/mole), E the modulus of elasticity, b the Burger's vector, σ_θ the applied hoop stress, $\dot{\varepsilon}_\theta^s$ the steady-state hoop creep rate, and RT has the usual meaning. Following Sherby's semi-empirical models [8], an exponential stress law was regarded as

appropriate here since at the present test conditions,

$$\sigma_\theta > 10^{-3}\ E \qquad \text{and} \qquad \dot{\varepsilon}^s_\theta > 10^9\ D, \tag{2}$$

where $D = 5 \exp(-62{,}000/RT)$ cm^2/s [6]. As shown in [1], the calculated creep rates using eq. (1) were in excellent agreement with the experimental data.

In correlating the primary creep behavior, the functional dependence for strain at any time t was found [1]:

$$\varepsilon_\theta - \varepsilon^o_\theta = f(\dot{\varepsilon}^s_\theta t) = F\left(\frac{A_1 DEb}{kT} \exp\ (B_1\sigma_\theta/E)t\right) \tag{3}$$

where ε_θ is the time-dependent plastic strain, and ε^o_θ is the initial loading strain at t = 0. Eq. (3) implies that data at different temperatures and stresses, when plotted as $(\varepsilon_\theta - \varepsilon^o_\theta)$ versus $\dot{\varepsilon}^s_\theta t$, should converge into a single universal curve described by the function f. Figure 1 is a plot of the net plastic strain versus weighted time illustrating the universal creep behavior. Murty, et al.[1], suggested an Avrami-type equation, derived from the first principles, which approximately described the universal curve. The following equation is seen to predict the curve more accurately (Figure 1):

$$\varepsilon_\theta = \varepsilon^o_\theta + \frac{1 + A + AB\dot{\varepsilon}^s_\theta t}{1 + AB\dot{\varepsilon}^s_\theta t}\ \dot{\varepsilon}^s_\theta t\,. \tag{4}$$

A and B are material constants in eq. (4), and

$$A = \dot{\varepsilon}^i_\theta/\dot{\varepsilon}^s_\theta, \qquad \text{and} \qquad B = 1/\varepsilon_T, \tag{5}$$

where $\dot{\varepsilon}^i_\theta$ is the initial creep rate at t = 0, and ε_T is the extent of the primary creep.

3. Anelastic Strain Formulation

Nir, et al. [4], proposed that a sudden change in the applied stress results in short-term anelastic deformation in addition to the time-dependent plastic flow. Anelastic strain is defined as time-dependent, recoverable deformation in contrast to the permanent plastic deformation, which is not recoverable. Thus, the total anelastic strain change accomplished after each load change is completely reversible upon reversing the sign of the load change. This anelastic component of the total strain reaches a saturation value that is determined solely by the new stress value. The following nonlinear relationship for the anelastic strain rate was proposed [3-5]:

$$\dot{a} = \dot{a}^*(a_s - a)^M \tag{6}$$

where $\dot{a}^*$ and M are material constants and have the same meaning as in the equation of state proposed by Hart [3,4]. In eq. (6), $\dot{a}$ is the anelastic strain rate at time t, a is the anelastic strain at t, and a_s is the saturation value that depends on the level of the new stress. Integration of eq. (6) yields

$$(a_s - a_o)^{1-M} - (a_s - a)^{1-M} = (1-M)\dot{a}^*(t - t_o) \tag{7}$$

where a = anelastic strain at t, and t_o = time at which stress was changed from σ_o to σ_s. Following Hart, et al. [3,5], an anelastic modulus is defined so that

$$a_o = \sigma_o/\mu, \qquad a_s = \sigma_s/\mu. \tag{8}$$

The anelastic modulus μ can be determined from stress drop tests [5]. By letting

$$\nu = M - 1, \tag{9}$$

eq. (7) can be rewritten to yield the following expression for the anelastic strain a at any time t,

$$a = a_s - [(a_s - a_o)^{-\nu} + \nu \mathring{a}^*(t - t_o)]^{-1/\nu}. \tag{10}$$

Figure 2 is a schematic representation of the variation of the anelastic strain with time predicted by eq. (10).

4. Strain Transients Following Stress Changes

The formulation above for the anelastic strain following a stress change is used in the present analysis. The total strain (ε) at any time t is given by

$$\varepsilon = \varepsilon_E + \alpha + a. \tag{11}$$

Here ε_E is the elastic strain ($= \sigma/E$), and α is the plastic strain given by $(\varepsilon_\theta - \varepsilon_\theta^o)$ in eq. (4), which consists of the primary as well as the secondary creep contributions. Using eq. (10), the anelastic strain component a is evaluated from

$$a = \pm\left\{[|a_s - a_o|^{-\nu} + \nu \mathring{a}^*(t - t_o)]^{-1/\nu} - |a_s - a_o|\right\}, \tag{12}$$

where t_o is the time at which the stree was changed from σ_o to σ_s; minus for stress increase ($\sigma_s > \sigma_o$), and plus for stress decrease ($\sigma_s < \sigma_o$). A plot of eq. (12) is shown in Figure 3.

The plastic strain component α at the new stress level was evaluated using eq. (4). The existence of a single master curve (Figure 1) describing creep at the temperatures and stresses employed here implies that the microstructures developed during creep at any given strain are identical irrespective of the test conditions, and thus the strain-hardening rule (in lieu of time-hardening) is regarded appropriate and will be used in the present analyses.

Closed-end internal pressurization tests were conducted on cold-worked, stress-relieved Zircaloy-4 cladding at a constant temperature of 750F (671.9K) and the hoop strains were continuously monitored using extension arm LVDT extensometers. The hoop stress change was accomplished by suddenly changing the internal pressure at a prescribed time, and the stress change was completed in less than 15 seconds. Figure 4 shows an example of the hoop creep strain versus exposure time where the sample was first crept at 15 ksi; after about 115 hours' exposure, the stress was increased to 25 ksi. At a total exposure period of about 143 hours, the stress was dropped to 15 ksi and the sample was crept for a total of 380 hours, at which time it was unloaded. Two significant features are apparent: decreased primary creep region after a stress increase and negative (inverse) transient creep following a stress drop. It should be noted that inverse transeints are observed due to a significant stress drop after lare (about 1%) prior creep strain; smaller stress drops revealed either reduced normal or zero creep transients.

The model equations described earlier can be readily applied to the example above. Hart and coworkers [3-5] observed that a value of 8 for M is applicable for all metallic systems, and Huang, et al. [9], reiterated the same for annealed Zircaloy. $\mathring{a}^*$ was determined by Huang, et al. [9], using load relaxation tests on Zircaloy cladding. The anelastic modulus μ was determined from closed-end internal pressurization creep tests where the hoop stress was

decreased to zero after prior creep while continuously monitoring the diametral strain. The following parameters were regarded applicable for the present case:

$$M = 8, \qquad \dot{a}^* = 2.52 \times 10^{22}, \qquad \mu = 15 \times 10^6 \text{ psi}. \tag{13}$$

The model predictions, along with the experimental data of the test described above, is shown in Figure 4. Excellent agreement is seen between the model predictions and the experimental observations. A noteworthy feature is the prediction of the transients, in particular the negative creep following the load drop from 25 to 15 ksi at 145 hours' exposure. Similar results and agreements were observed at other test conditions.

5. Creep Under Cyclic Loading

In order to check the applicability of the proposed model equations for creep under cyclic loading, uniaxial creep tests were conducted on Zircaloy tubing using a hydraulic, closed-loop Instron machine. The applied load was cycled between the prescribed minimum and maximum loads with the Instron machine in load-control, while monitoring the axial strain continuously using an axial LVDT extensometer. Again the testing was carried out at 750F. Relatively higher stresses were employed to reduce the testing time. Since the mechanical properties of Zircaloy cladding are highly anisotropic [10], the constants in equations (1) and (4) were re-evaluated from axial creep tests covering the stress range employed in the cyclic creep tests. As seen in Figure 5, the model predictions are in excellent agreement with the experimental data. Essentially the same constants as in eq. (13) were used for the anelastic strain evaluation. Since, at the temperature and stress range employed here, creep in Zircaloy-4 is diffusion-controlled [1], such an agreement between the model predictions and experimental meausrements is not surprising. It should be noted [11] that such a simple extension to cyclic creep may not be valid at low enough temperatures where creep is not diffusion-controlled.

6. Extension to Multiaxial Creep

It is proposed that the present model equations may be extended to describe multiaxial creep strains under multiaxial loading. From considerations based on generalized stress formulations in terms of the anisotropy parameters R and P [10], it can be shown that [12]

$$\begin{pmatrix} \dot{\varepsilon}_r \\ \dot{\varepsilon}_\theta \\ \dot{\varepsilon}_z \end{pmatrix} = \frac{\dot{\varepsilon}_g}{P(R+1)\sigma_g} \begin{pmatrix} R+P & -R & -P \\ -R & R(P+1) & -PR \\ -P & -PR & P(R+1) \end{pmatrix} \begin{pmatrix} \sigma_r \\ \sigma_\theta \\ \sigma_z \end{pmatrix} \tag{14}$$

where

$\dot{\varepsilon}_g$ = generalized strain rate, $\dot{\varepsilon}_\theta$ = hoop strain rate,
σ_g = generalized stress, σ_θ = hoop stress,
$\dot{\varepsilon}_r$ = radial strain rate, $\dot{\varepsilon}_z$ = axial strain rate,
σ_r = radial stress, σ_z = axial stress.

For a given stress state (σ_r, σ_θ, σ_z) the generalized stress (σ_g) is given by Hill's equation:

$$\sigma_g = \sqrt{\frac{R(\sigma_r - \sigma_\theta)^2 + RP(\sigma_\theta - \sigma_z)^2 + P(\sigma_z - \sigma_r)^2}{P(R+1)}}. \tag{15}$$

Thus, from eqs. (14) and (15) it follows that the functional dependence of $\dot{\varepsilon}_g$ on σ_g is

identical to that of $\dot{\varepsilon}_z$ on σ_z in a uniaxial axial ($\sigma_r = 0 = \sigma_o$) creep test. Thus, in equations (1), (4), and (10), the appropriate strain rates and stress will be $\dot{\varepsilon}_g$ and σ_g, and the verious material constants will be modified by the appropriate anisotropy parameters. Multiaxial creep experiments and correlations with the model predictions are underway and will be published elsewhere.

7. Summary and Conclusions

The model equations developed in the past [1], based on climb-controlled dislocation slip, for creep under constant loads were extended to describe the transients following load changes. The accumulated strain at any instant is given by the sum of the elastic, anelastic and plastic strain components. The anelastic strain component was modeled after Hart, et al. and strain-hardening rule was used in evaluating plastic strain following the stress change. Closed-end internal pressurization creep tests were carried out on cold-worked, stress-relieved Zircaloy-4 cladding tubes while continuously monitoring the diametral strains. Using the constants experimentally evaluated from constant-stress creep and load relaxation tests, a good correlation was noted between the model predictions and experimental measurements. The proposed model accurately predicted the experimentally observed inverse (negative) creep transients following a significant drop in the applied stress.

The present model equations are also shown to yield an excellent correlation with cyclic creep data. Uniaxial creep tests were conducted on a closed-loop hydraulic Instron machine under cyclically varying loads. The experimental axial strain data were seen to be in excellent agreement with the model predictions.

Extensions of the proposed model equations to describe the anisotropic multiaxial creep behavior under varying multiaxial stresses are outlined.

Acknowledgments

Various discussions with Professor Che-Yu Li of Cornell University and Mr. B. L. Adams and the constant encouragement of Dr. G. S. Clevinger and Mr. L. J. Ferrell are gratefully acknowledged. Acknowledgments are due Mr. W. T. Hamilton, Jr., for skillful assistance in the experiments. This work was sponsored by the Nuclear Power Generation Division of The Babcock & Wilcox Company.

References

[1] MURTY, K. L., CLEVINGER, G. S., PAPAZOGLOU, T. P., Thermal Creep of Zircaloy-4 Cladding," Trans. 4th Intl. Conf. on SMIRT, August 1977, Paper C3/4.

[2] BAYCE, A. E., et al., "Effect of Stress on the Creep of Aluminum in the Dislocation Climb Range," Trans. ASM, 52 (1960), p. 451.

[3] HART, E. W., "Constitutive Relations for the Nonelastic Deformation of Metals, Trans. ASME, J. Engrg. Mater. & Technology, 98H (1976), p. 193.

[4] HART, E. W., LI, CHE-YU, "use of State Variables in the Description of Irradiation Creep and Deformation of Metals," ASTM STP633 (1977), p. 315.

[5] NIR, N., HART, E. W., LI, CHE-YU, "Anelastic Deformation of High Purity Aluminum at Room Temperature," Scripta Met., 10 (1960), p. 189.

[6] LYASHENKO, V. S., BYKOR, V. N., PAVLINOV, L. V., "A Study of Self-Diffusion in Zirconium and its Alloys with Tin," Fiz. Metalle Metalloved, 8 (1959), p. 362; Phys. Metals Metallograph (1960), p. 40.

[7] BIRD, J. E., MUKHERJEE, A. K., DORN, J. E., in Quantitative Relation Between Properties and Microstructure, Israel University Press (1969), pp 255-342.

[8] SHERBY, O. D., BURKE, P. M., "Mechanical Behavior of Polycrystalline Solids at Elevated Temperature," Prog. Mat. Sci., 13 (1967), p. 325.

[9] HUANG, F. H., et al., "Load Relaxation Studies of Zircaloy-4," J. Nucl. Materials, 79 (1979), p. 214.

[10] BEAUREGARD, R. J., CLEVINGER, G. S., MURTY, K. L., "Effect of Annealing Temperature on the Mechanical Properties of Zircaloy-4 Cladding," Trans. 4th Intl. Conf. on SMIRT, August 1977, Paper C3/5.

[11] Private Communication from Professor Che-Yu Li of Cornell University.

[12] CLEVINGER, G. S., ADAMS, B. L., MURTY, K. L., "Analysis of Irradiation Growth and Multi-axial Deformation Behavior of Nuclear Fuel Cladding," 4th Intl. Conf. on Zirconium in the Nuclear Industry, Stratford-on-Avon, England, June 1978.

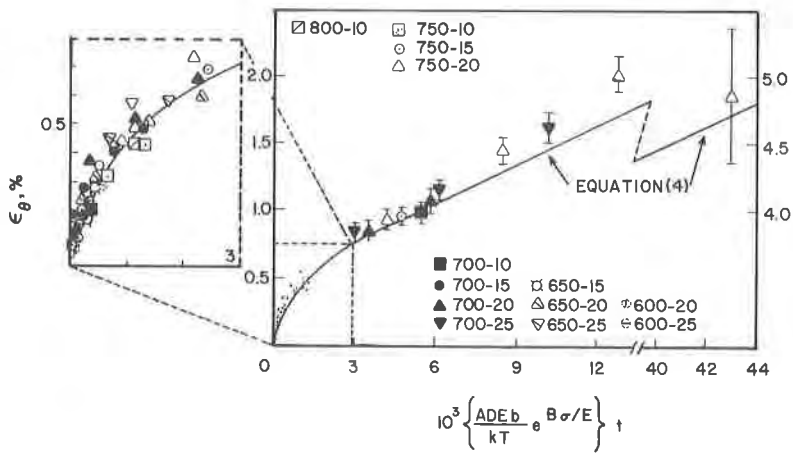

Figure 1. Creep Strain Vs Weighted Time Illustrating Universal Behavior and Comparison With Theory

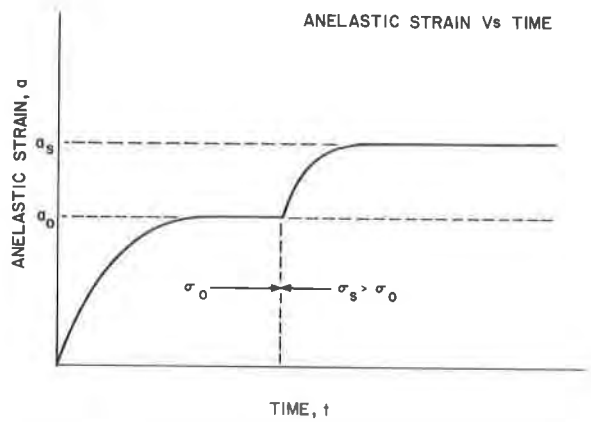

Figure 2. Anelastic Strain Vs Time [Equation (10)]

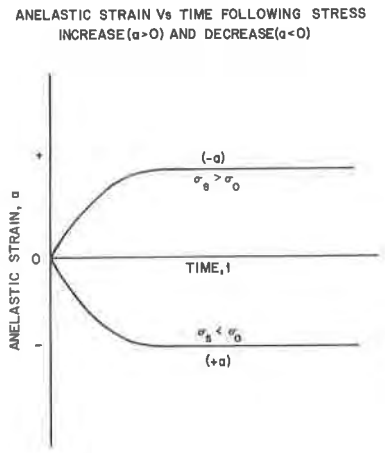

Figure 3. Time Dependence of Anelastic Strain Following Stress Increase (a > o) and Decrease (a < o)

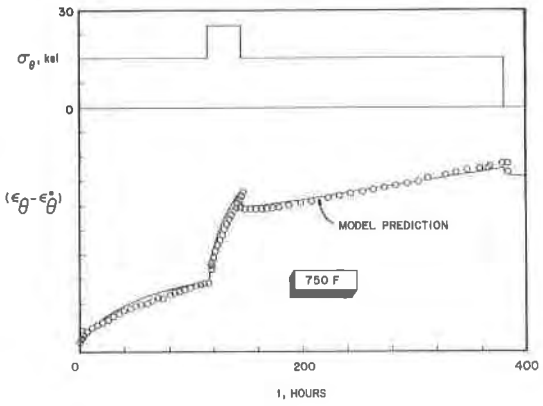

Figure 4. Hoop Creep Curve Depicting Transients Due to Stress Change at 750F [Model Predictions (——) Compared With Experimental Data (ooo)]

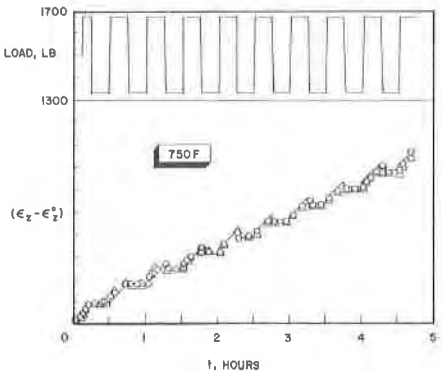

Figure 5.
Uniaxial Creep Curve Under Cyclic Loading at 750F [Comparison of Experimental Data (ooo) With Model Predictions (——)]